International Journal of Bifurcation and Chaos, Vol. 17, No. 10 (2007) 3613–3617

DISCRETE DYNAMICAL SYSTEMS CONSISTING OF SINGLE-ELECTRON CIRCUITS

ANDREW KILINGA KIKOMBO*, TAKAHIDE OYA, TETSUYA ASAI
and YOSHIHITO AMEMIYA
Department of Electrical Engineering, Hokkaido University,
Kita 13, Nishi 8, Sapporo 060-8628, Japan
**kikombo@sapiens-ei.eng.hokudai.ac.jp*

Received October 18, 2005; Revised March 31, 2006

The single-electron circuit in the nature of discrete dynamical systems because it changes its state discontinuously because of electron tunneling. To confirm this, we designed a sample circuit consisting of two single-electron oscillators coupled with each other through a coupling capacitor. The oscillators produce relaxation oscillation and interact with each other to generate synchronization and entrainment. The operation of the circuit is expressed with a set of discrete difference equations combined with continuous differential equations. Computer simulation shows that the circuit exhibits a variety of periodic oscillations and produces a series of bifurcations as the coupling capacitance increases.

Keywords: Single-electron circuit; coupled oscillator; discrete dynamical system; bifurcation.

1. Introduction

The single-electron circuit is an electronic circuit designed to produce electronic functions by controlling the transport of individual electrons. Unlike ordinary circuits, it changes its internal state discontinuously, producing nonlinear oscillations in which discrete-time and continuous-time dynamics coexist. This paper demonstrates such complex behavior of single-electron circuits.

A single-electron circuit has a number of nodes that are interconnected with tunneling junctions. Electrons in each node can tunnel to another node through the tunneling junction, and each individual tunneling can be controlled by making use of the Coulomb blockade phenomenon. A detailed explanation is given by Gravert and Devoret [1992] and Wasshuber [2001]. Through electron tunneling, a single-electron circuit discontinuously changes its internal state (or distribution of electrons among the nodes), thereby making a discontinuous change in its node voltages. Single-electron circuits consequently act as a compound of discrete and continuous dynamical systems.

In the following sections, we first consider a simple oscillator, the single-electron tunneling cell, with its relaxation oscillation induced by electron tunneling. Then we examine a sample device consisting of two oscillators coupled with each other and demonstrate its complex dynamics, a variety of periodic oscillations and a series of bifurcations, by means of computer simulation.

2. Single-Electron Oscillator

An elementary component of single-electron circuits is the single-electron tunneling cell shown in Fig. 1(a). It consists of a tunneling junction (capacitance = C_0) and a high resistance R_0 connected in series at node 1 and biased with a positive power voltage V_{dd}. This single-electron cell was proposed by Likharev *et al.* [1985] and its nonlinear dynamics were studied by Averin *et al.* [1986]

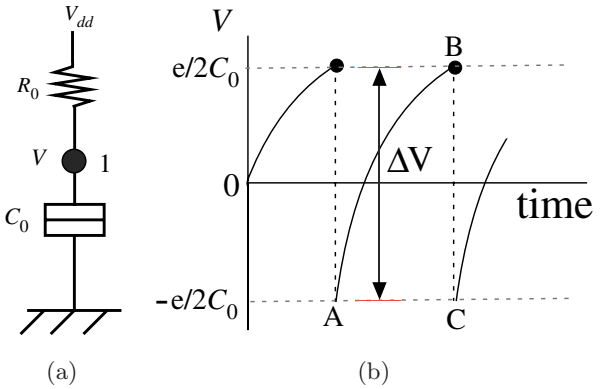

Fig. 1. (a) Single-electron cell consisting of a tunneling junction C_0 and a resistance R_0 connected in series at node 1, and biased with a positive power voltage V_{dd}. (b) Waveform of the oscillation in voltage V at node 1, consisting of continuous curve AB and discontinuous drop BC.

and Fulton *et al.* [1987]. The cell operates as an oscillator if $V_{dd} > e/(2C_0)$ (e is the elementary charge) and produces a relaxation oscillation at low temperatures at which the Coulomb blockade occurs. Figure 1(b) shows the waveform of the oscillation of voltage V at node 1. The node voltage gradually increases as junction capacitance C_0 is charged through resistance R_0. When the voltage reaches the threshold voltage $e/(2C_0)$, it drops discontinuously to $-e/(2C_0)$ because of an electron tunneling from the ground to node 1 through the junction. After the discontinuous change of voltage, the node voltage gradually increases repeating the same cycle. The dynamics is given by a combination of continuous differential equation,

$$\frac{dV}{dt} = \frac{V_{dd} - V}{R_0 C_0} \tag{1}$$

for charging curve AB, and discrete difference equation,

$$\Delta V = \frac{e}{C_0}, \tag{2}$$

for the discontinuous drop BC, where ΔV is the difference in the node voltage before and after tunneling (also see Appendies A and B).

3. Coupled Single-Electron Oscillators

Single-electron oscillators will exhibit complex dynamics when they are coupled with one another. As an example of such coupled oscillators, we propose a circuit consisting of two single-electron oscillators coupled with each other. Figure 2 shows the circuit configuration. One oscillator consists of a

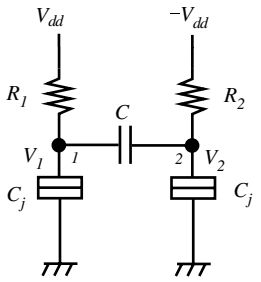

Fig. 2. Coupled single-electron oscillator consisting of two tunneling cells coupled through capacitance C and biased with positive and negative power voltages V_{dd} and $-V_{dd}$.

resistor R_1 and a left tunneling junction C_j biased with a positive voltage V_{dd}. The other oscillator consists of a resistor R_2 and a right tunneling junction C_j biased with a *negative* voltage $-V_{dd}$. The two oscillators are coupled with each other at nodes 1 and 2 through a coupling capacitor C. The variables of the circuit are node voltages V_1 and V_2. The threshold of the junction voltages for tunneling is $\pm(C+C_j)/(2C_j(2C+C_j))$ for this circuit, and electron tunneling occurs through the corresponding junction if either of the node voltages reaches the threshold.

Coupled through capacitor C, the two oscillators interact with each other to produce synchronization and entrainment. Figure 3 depicts an example of the operation on a V_1–V_2 phase plane. Node voltages V_1 and V_2 change continuously as the junction capacitances are charged through the resistances. When either of the node voltages reaches the threshold, tunneling occurs through the corresponding junction, and this causes a discrete change in both node voltages. For instance, the

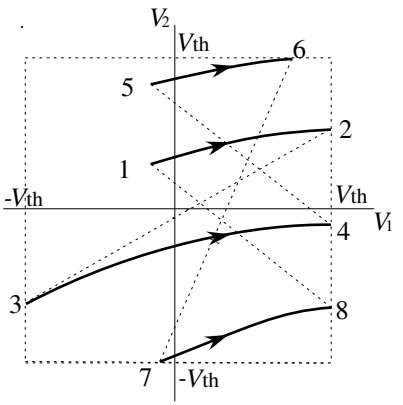

Fig. 3. Schematic trajectory of the oscillation in the coupled oscillators, plotted on a V_1–V_2 phase plane. Dashed lines show a discrete change caused by tunneling.

trajectory of oscillation starts at point 1, proceeds rightward to 2, then it jumps discontinuously to 3 because of electron tunneling in the left junction, proceeds to 4, jumps to 5 (tunneling in the left junction, followed by immediate tunneling in the right junction), proceeds to 6, jumps to 7 (tunneling in the right junction), proceeds to 8, and finally returns to 1 (tunneling in the left junction, followed by immediate tunneling in the right junction). Thus, the circuit produces a periodic oscillation in which discrete-time and continuous-time dynamics coexist.

4. Simulating the Dynamics of the Coupled Oscillators

4.1. *Expression for the dynamics of the circuit*

To express the dynamics of the coupled oscillators, we rewrote the variables and parameters by using equations,

$$u = \frac{2C_0}{e}V_1, \quad v = \frac{2C_0}{e}V_2,$$
$$C_0 = \frac{(2k+1)}{(k+1)}C_j, \quad k = \frac{C}{C_j}, \tag{3}$$
$$\alpha = \frac{R_2}{R_1}, \quad \beta = \frac{2C_0}{e}V_{dd}, \quad \text{and} \quad t = \frac{\text{time}}{R_1C_0}.$$

where, u and v are normalized node voltages, k is the coupling coefficient ($k \geq 0$), α is the resistance ratio ($\alpha > 1$), β is normalized bias power voltage ($\beta > 0$), and t is normalized time. The dynamics of the circuit, which depend entirely on the dimensionless parameters α, β and k, can be expressed with a trajectory on a u–v phase plane. Taking into account the Coulomb blockade, we obtained the following equations for the dynamics. The normalized threshold voltage for tunneling is ± 1. The operation is continuous-time in a range of $-1 < u < 1$ and $-1 < v < 1$ and is given by differential equations,

$$\frac{du}{dt} = (\beta - u) - \frac{k}{k+1}\frac{1}{\alpha}(\beta + v), \tag{4}$$

$$\frac{dv}{dt} = \frac{k}{k+1}(\beta - u) - \frac{1}{\alpha}(\beta + v). \tag{5}$$

When either u or v reaches the threshold ± 1, tunneling occurs in the corresponding junction and node voltages u and v change discretely by Δu and Δv, where

$$\begin{aligned}
&\Delta u = -2 \quad \text{and} \quad \Delta v = -\frac{2k}{k+1} \ \text{ if } u \text{ reaches } 1,\\
&\Delta u = 2 \quad \text{and} \quad \Delta v = \frac{2k}{k+1} \ \text{ if } u \text{ reaches } -1,\\
&\Delta u = -\frac{2k}{k+1} \quad \text{and} \quad \Delta v = -2 \ \text{ if } v \text{ reaches } 1,\\
&\Delta u = \frac{2k}{k+1} \quad \text{and} \quad \Delta v = 2 \ \text{ if } v \text{ reaches } -1.
\end{aligned} \tag{6}$$

4.2. *Attractors on the u–v phase plane*

We simulated the operation of the coupled oscillators for sample sets of parameters and plotted the trajectory of the oscillation on u–v phase planes. The trajectory depended on initial values of u and v but was attracted, as time passed, to a set of curves (i.e. the attractor of the oscillation) independent of the initial values. Figures 4(a) through 4(d) show the attractor for $\alpha = \sqrt{10}$ and $\beta = 3$, with coupling coefficient k as a parameter. As the figures show, a slight change in the coupling coefficient produces a drastic change in oscillation cycle.

The flow of the attractor can be simply expressed with the values of v at which segments of the attractor meet line $u = 1$. For instance, the flow in Fig. 4(b) can be expressed with a sequence of 17 values of v. This is one kind of Poincare map, and no information is lost in terms of the qualitative behavior of the dynamics. We used the set of these v values to draw bifurcation diagrams in the next section. We refer to the number of these v values as the degree of periodicity in oscillation.

4.3. *Effect of the coupling coefficient and the resistance ratio on the dynamics*

To come up with a general view of the effect of coupling coefficient k and resistance ratio α on the dynamics, we drew bifurcation diagrams by plotting the set of the v values as a function of k and α. Figure 5 shows a bifurcation diagram with k as a bifurcation parameter. The resistance ratio was set to $\alpha = 3$ for (a) and $\alpha = \sqrt{10}$ for (b), and the bias power voltage was $\beta = 3$ for both diagrams. At $k = 0$ (without coupling), the two oscillators in the circuit produced a self-induced oscillation independent of each other. As coupling coefficient k increased, the oscillators began to interact with

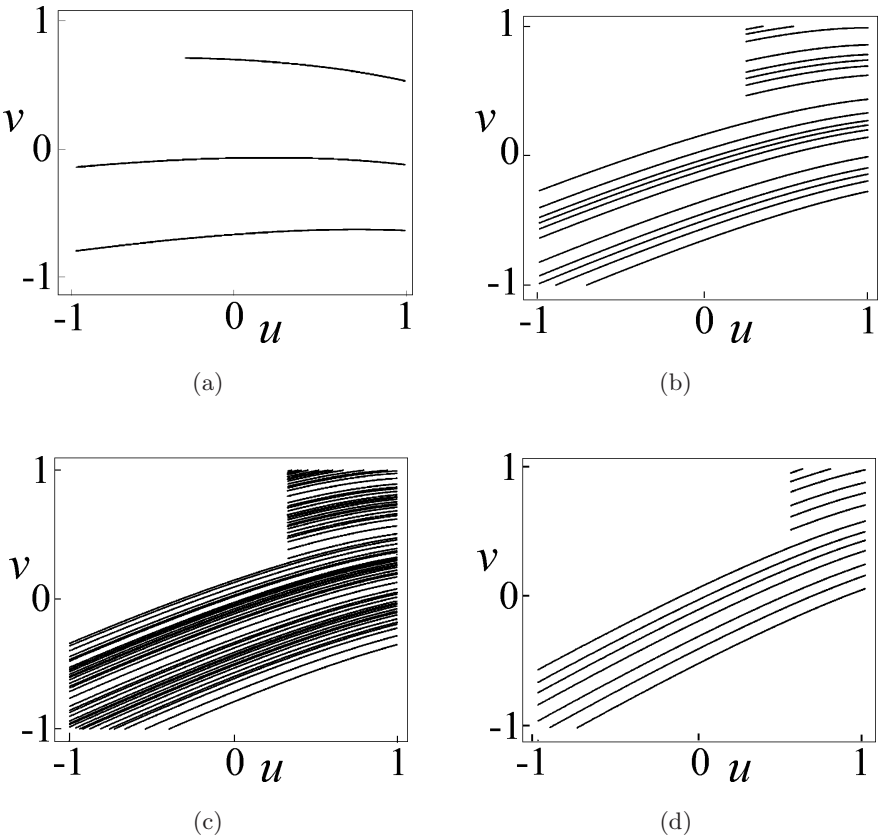

Fig. 4. Attractors of the oscillation plotted on a u–v plane, simulated with coupling coefficients (a) $k = 0.5$ (3-cycle oscillation), (b) $k = 1.7$ (19-cycle), (c) $k = 2$ (58-cycle), and (d) $k = 3.5$ (13-cycle). The resistance ratio $\alpha = \sqrt{10}$ and bias power voltage $\beta = 3$ for all figures.

each other to produce entrainment and synchronized periodic oscillation. Generally speaking, the degree of periodicity increased with the increase of k. However there were many windows where the degree of periodicity decreased drastically. The windows appeared irregularly and repeatedly.

Figures 6(a) and 6(b) show the bifurcation diagram with resistance ratio α as a bifurcation parameter. The coupling coefficient and the power voltage were set to $k = 0.2$ for (a) and $k = 1$ for (b), with $\beta = 3$ for both diagrams. The degree of periodicity increased as α increased, but windows also appeared repeatedly. In each window, the degree of periodicity is equal to the nearest integer value of α.

In summary, the circuit showed a variety of nonlinear, periodic oscillations in which discrete-time and continuous-time dynamics coexist, and the degree of periodicity increased rapidly as the

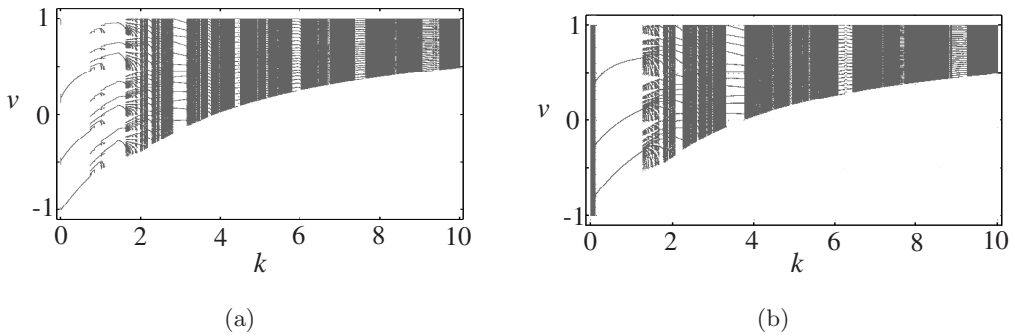

Fig. 5. Bifurcation diagram with coupling coefficient k as a parameter. Resistance ratio is (a) $\alpha = 3$ and (b) $\alpha = \sqrt{10}$. Power voltage $\beta = 3$ for both diagrams.

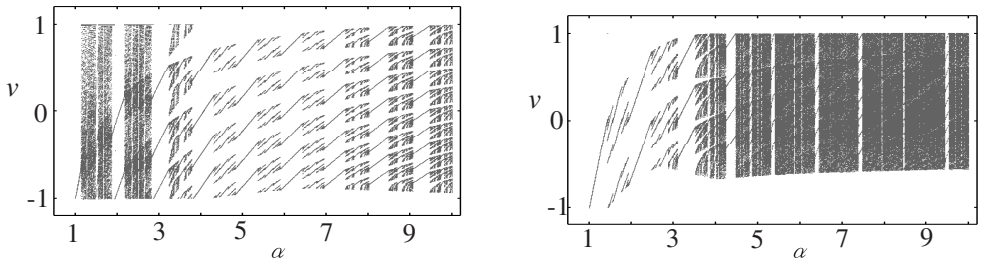

Fig. 6. Bifurcation diagram with resistance ratio α as a parameter. The coupling coefficient is (a) $k = 0.2$ and (b) $k = 1$. Power voltage $\beta = 3$ for both diagrams.

coupling coefficient (and the resistance ratio) increased. However, we have yet to make certain of chaotic operation. We are now studying to confirm whether chaos appears in our coupled-oscillator circuit.

References

Averin, D. V. & Likharev, K. K. [1986] "Coulomb blockade of single-electron tunneling, and coherent oscillations in small tunnel junctions," *J. Low Temp. Phys.* **62**, 345–373.

Wasshuber, C. [2001] *Computational Single-Electronics* (Springer-Verlag, Wien, NY).

Fulton, T. A. & Dolan, G. J. [1987] "Observation of single-electron charging effects in small tunnel junctions," *Phys. Rev. Lett.* **59**, 109–113.

Gravert, H. & Devoret, M. H. [1992] *Single Charge Tunneling* (Plenum Press, NY).

Kamakura, K., Motohisa, J. & Fukui, T. [1997] "Formation and characterization of coupled quantum dots (CQDs) by selective area metalorganic vapor phase epitaxy," *J. Crystal Growth* **170**, 700–704.

Likharev, K. K. & Zorin, A. B. [1985] "Theory of the Bloch-wave oscillations in small Josephson junctions," *J. Low Temp. Phys.* **59**, 347–382.

Oya, T., Asai T., Fukui, T. & Amemiya, Y. [2002] "A majority-logic nanodevice using a balanced pair of single-electron boxes," *J. Nanosci. Nanotech.* **2**, 333–342.

Takeda, J., Akabori, M., Motohisa, J., Notzel, R. & Fukui, T. [2005] "Selective-area MOVPE fabrication of GaAs hexagonal air-hole arrays on GaAs(111)B substrates using flow-rate modulation mode," *Nanotechnology* **16**, 2954–2957.

Appendix A

Waiting Time

Strictly speaking, a time lag or a waiting time exists between when junction voltage exceeds tunneling threshold $e/(2C_0)$ and when tunneling actually occurs. This is caused by the stochastic nature of tunneling, and the waiting time has probabilistic fluctuations in every tunneling event. However, we have confirmed through theoretical analysis that the effect of waiting time decreases to zero as resistance R in the circuit increases. We can ignore the waiting time if we use a sufficiently large resistance. The situation is the same in the coupled oscillators described in Sec. 3.

Appendix B

Device Fabrication

Several nanotechnologies have been proposed to fabricate single-electron devices on a semiconductor substrate. One promising method is to use the selective-area MOVPE technique reported by Kumakura *et al.* [1997] and Takeda *et al.* [2005]. For a fabrication process for single-electron oscillators, see Oya *et al.* [2002].